

Investigation of the Growth Mechanism of an InSe Epitaxial Layer on a MoS₂ Substrate

Toshiyuki Hayashi, Keiji Ueno^{*}, Koichiro Saiki^a and Atsushi Koma

Department of Chemistry, The University of Tokyo

^a Department of Complexity Science and Engineering, The University of Tokyo

7-3-1 Hongo, Bunkyo-ku, Tokyo 113-0033, Japan

Abstract

Sub-monolayer films of layered semiconductor InSe were grown on MoS₂ substrates by molecular beam epitaxy, and the change in their growth features with Se/In flux ratio was investigated using scanning tunneling microscope in vacuum. It was found that InSe domains grown at 340 °C have a hexagonal shape when the Se/In ratio is about 17. Detailed images of the hexagonal InSe domains have revealed that adjacent sides of the hexagon have different structures; one is a straight edge and the other is a disordered edge. When the Se/In ratio was decreased, the disordered edges became predominant, the straight edges disappeared, and the InSe domain became triangular. Contrary, when the Se/In ratio was increased, InSe domains became triangular ones consisting of only straight edges. The growth mechanism of InSe domains is discussed by considering the crystal structure of InSe and the reactivity of each side with incoming atoms. It is suggested that the balance of incorporation rate of In and Se atoms determines the structure of InSe domains.

PACS: 61.16.Ch, 68.10.Jy, 68.35.Fx

KEYWORDS: STM, layered material, InSe, MoS₂, growth kinetics

* Corresponding author:

Tel: +81-3-5841-4354 FAX: +81-3-5689-0654

E-mail: kei@chem.s.u-tokyo.ac.jp

1. Introduction

Investigation of the growth mechanism of thin films grown by molecular beam epitaxy (MBE) has shown remarkable progress during the last decade owing to development of scanning tunneling microscopy (STM) and atomic force microscopy (AFM) [1, 2]. Real-space high-resolution images of STM and AFM have enabled us to see the process of nucleation at the early stage of the growth. They are also useful to observe the structure of growing domains, the surface reconstruction, defects and dislocations in the grown film. It is difficult to observe the surface by STM or AFM under the MBE growth, but reflection high-energy electron diffraction (RHEED) observation, for example, gives complementary information on the growth mechanism.

In this paper, we report the STM investigation on the growth mechanism of an InSe thin film grown on a MoS₂ substrate. Both InSe [3] and MoS₂ [4] have lamellar crystal structures as shown in Figs. 1 (a) and (b), respectively. They consist of two-dimensional unit layers bound together by weak van der Waals-like force. No dangling bond appears on cleaved surfaces of InSe and MoS₂ so that their surfaces are very inactive. Then it is possible to grow a single-crystalline epitaxial film of InSe on a MoS₂ substrate in spite of large differences in the lattice constant and the crystal structure. This comes from the fact that there are no strong interfacial bonds which introduce distortion into the grown film. We named this type of heteroepitaxy “van der Waals epitaxy (VDWE)” [5], and many experimental evidences that layered materials can be

grown on foreign layered materials independent of the lattice mismatch have been shown by us and some other groups [6-10].

Until now, the growth mechanism of VDWE has been investigated for the MBE-grown GaSe/MoS₂ system using RHEED and AFM [11, 12]. The RHEED observation proved that a monolayer GaSe film grows on a MoS₂ substrate with its *c*-axis perpendicular to the substrate, and with its *a*-axis parallel to that of the substrate. AFM images with atomic resolution indicated that the initial layer of GaSe has the same Se-Se atomic interval as that of a bulk GaSe in spite of the large lattice mismatch (~19%) between GaSe and MoS₂. It was also revealed that all of monolayer GaSe domains grown at the substrate temperature about 500 °C have a triangular shape [12].

The unit layer of InSe has the same crystal structure as GaSe, but the Se-Se interatomic distance on the InSe surface is larger than that of GaSe, and the lattice mismatch with MoS₂ is about 27%. We have grown InSe films under various growth conditions using separate molecular sources, and observed the change in growth feature by STM. Previously other groups have reported the STM observation of InSe films grown on GaSe [13, 14], but they reported only the surface morphology of grown films without considering the detailed growth mechanism of InSe. Our STM investigation has elucidated details of the growth mechanism and defect structures of InSe, which has not been fully understood by our previous AFM investigation [15, 16].

2. Experimental

The growth of InSe films was performed in an ultrahigh vacuum (UHV) MBE chamber with base pressure of 2×10^{-8} Pa. MoS₂ substrates of about $5 \times 5 \times 0.2$ mm³ were cut from natural molybdenite specimens. They were cleaved in air just before loading into the chamber, and thermally cleaned by heating at 500 °C for 30 min under UHV. Elemental indium (99.9999%) and selenium (99.9999%) were evaporated from separate Knudsen cells, and the beam equivalent pressure (BEP) of In and Se fluxes was monitored by a movable nude ion gauge at the same position with the substrate. After cleaning the MoS₂ surface, In and Se beams were irradiated onto the substrate at the substrate temperature of 340 °C. In the present experiment, BEP of In flux was fixed to 3.0×10^{-6} Pa, and BEP of Se flux was changed from 2.0×10^{-5} Pa to 2.0×10^{-4} Pa, which corresponded to the Se/In BEP ratios 6.7 and 67, respectively. The surface of InSe films was monitored by RHEED during the growth. The growth was stopped when streaks in the RHEED pattern of the growing InSe film became as bright as those of the MoS₂ substrate. This corresponds to the coverage of about 0.6 ~ 0.8 monolayer (ML) InSe film, which was proved by our previous AFM experiments [15, 16].

Grown samples were taken out of the MBE chamber and observed by a UHV-STM apparatus with base pressure of 5×10^{-8} Pa. The samples were transferred by using a portable vacuum vessel, which prevented the sample from being exposed to the air. Electrochemically polished polycrystalline tungsten

wires were used as STM tips. All images were taken in the constant current mode. The tunneling current was set to 80 pA, and the sample bias voltage was changed for each STM image as indicated in the figure caption. We obtained STM images with other conditions of the bias voltage and the tunneling current, and almost the same results were obtained about the structure of InSe domains.

3. Results and Discussion

Figure 2 shows RHEED patterns of a MoS₂ substrate (a, b) and an InSe film (c, d) grown with the Se BEP of 5×10^{-5} Pa. Figures 2(a) and 2(c) were observed from the azimuthal direction of $[11\bar{2}0]$ of the MoS₂ substrate, while Figs. 2(b) and 2(d) were observed from the $[10\bar{1}0]$ azimuth direction by rotating the sample by 30°. As shown in Figs. 2(c) and 2(d), interval of streaks coming from the grown InSe film is narrower than that of MoS₂, reflecting the larger lattice constant of InSe (0.400 nm) than that of MoS₂ (0.316 nm). Each interval of streaks coming from MoS₂ or InSe in Fig. 2(d) is $\sqrt{3}$ times larger than that in Fig. 2(c), and the same pattern as in Fig. 2(c) was observed again when the sample was rotated by 60°. These changes of RHEED patterns mean that the surface of the grown InSe film has the same six-fold symmetry with a bulk single crystal. It is also elucidated that the *a*-axis of the grown InSe film is parallel to that of the MoS₂ substrate with its *c*-axis perpendicular to the surface.

Thus, it is clearly shown that the epitaxial growth of an InSe film is achieved on the MoS₂ substrate in spite of the 27% lattice mismatch. After confirming the crystallinity and the surface morphology by RHEED, we observed the samples by UHV-STM.

Figure 3 indicates wide-area STM images of InSe films grown on MoS₂ substrates with different Se BEP. Triangular and hexagonal regions in STM images are InSe islands, and the rest is bare MoS₂ substrate surface. With the lowest Se BEP of 2×10^{-5} Pa (In/Se BEP ratio is 6.7), each InSe domain has a nearly triangular shape (Fig. 3(a)). When the BEP of Se was increased to 5×10^{-5} Pa (Se/In BEP ratio is 17), the domain shape changed into a hexagonal one, but it became triangular again when the BEP of Se was further increased to 2×10^{-4} Pa (In/Se BEP ratio is 67). An atomic lattice image as shown in Fig. 4 can be observed on the flat area of every InSe domain. Hexagonal lattice symmetry and an interval of the atomic corrugation indicated in Fig. 4 well correspond to those of the bulk InSe crystal, which also suggests the single-crystalline epitaxial growth of the InSe film.

It must be noted that STM images in Fig. 3 are distorted due to the anisotropy of the piezoelectric tube so that the triangular InSe domain in (c), for example, is not equilateral. The AFM observation using a well-calibrated piezoelectric tube [15, 16], however, has already revealed that triangular domains are all equilateral, and hexagonal domains have angles of 120°.

It is known that an α -In₂Se₃ crystal also has the layered structure, and that

the topmost Se layer has the hexagonal symmetry and the same Se-Se interval length of 0.400 nm as that of InSe [17]. Thus, there still remains a possibility that the difference in the domain structure observed in STM images reflects the presence of two different compound films, InSe and α -In₂Se₃. In order to identify the atomic composition of grown films, we measured Auger electron spectroscopy (AES) for three 1ML-thickness films grown with above-mentioned BEP conditions. Then it was confirmed that every film has a same atomic composition within an experimental error.

From STM images shown in Fig. 3, it was elucidated that there exist two types of domain edge structures, one is *straight* and the other is *disordered*. The InSe domain grown with the lowest Se/In BEP ratio is surrounded by disordered edges as is shown in Fig. 3(a). On the contrary, the InSe domain grown with the highest Se/In BEP ratio has only straight edges as is shown in Fig. 3(c). In the case of the medium Se/In BEP ratio, these two types of domain edges alternately appear so that the grown InSe island becomes hexagonal, as is clearly seen in Fig. 3(b). The surface of the InSe domain is very smooth near the straight edge, whereas the surface near the disordered edge seems to be rough. The inner region of every domain, however, is as smooth as the substrate surface and atomic lattice images can be observed as mentioned above. In the following subsections, we will discuss the origin of different domain shapes and edge types from the viewpoint of growth kinetics of the InSe thin film.

In addition, we will argue about the position of In atoms relative to the

topmost Se atoms in the monolayer InSe domain in *Sec. 3-4*, which cannot be determined only by the STM image of the domain surface. No change in the atomic image of the InSe surface was observed when tunneling bias voltage was changed. This suggests that the atomic corrugation shown in Fig. 4 only reflects the lattice and the electronic structure of the topmost Se atoms, while inner In atoms are not observed. However, the presence of the two types of InSe domain edges enabled us to clarify the stacking position of In and Se atomic layers in the monolayer InSe film, as described later.

3-1. Change in the InSe domain structure along with the change in Se/In flux ratio

As explained above, the Se/In flux ratio affects the shape of the monolayer InSe domain. This phenomenon is considered to relate with the crystal structure of InSe. The hexagonal InSe crystal plane has two different kinds of domain edges, indicated as ‘type-A edge’ and ‘type-B edge’ in Fig. 5. It is expected that incorporation rates of incoming In and Se atoms at the type-A edge are different from those at the type-B edge. An incoming Se atom joins with *one* In atom while an incoming In atom makes bonds with *two* Se atoms at the type-A edge. Contrary, at the type-B edge an incoming Se atom joins with *two* In atoms, while an incoming In atom makes a bond with *one* Se atom. It is not so obvious which of type A edge and type B edge is more active to incorporate Se atoms. But here we consider that incorporation rate of Se atoms at the type

B edge is faster than that at the type-A edge, since an incoming Se atom which connects with either of two In atoms may be eventually incorporated into the existing domain at the type-B edge.

When a large amount of Se atoms are supplied onto the substrate surface, the incorporation rate of Se atoms can be saturated both at the type-A and type-B edges of the InSe domain. Excess Se atoms re-evaporate from the surface at the substrate temperature of 340 °C, and have no contribution to the growth of the InSe domain. In this case, the growth rate of the InSe domain is determined by the incorporation rate of In atoms. As explained above, the incorporation rate of In atoms at the type-A edge is faster than that at the type-B edge, which results in the faster growth of the type-A edge than the type-B edge. Therefore, triangular InSe domains surrounded by the type-B edges grow when the Se/In BEP ratio is extremely high.

When the flux intensity of Se is decreased and it becomes below the saturation condition at the type-A edge, the incorporation rate of Se atoms begins to determine the growth speed of the type-A edge. The type-B edge, however, is still saturated with Se atoms and the growth speed of the type-B edge is still determined by the incorporation rate of In atoms, because this edge reacts with Se atoms more strongly than the type-A edge. Under this condition the growth speed of the type-A edge becomes slower, and it becomes comparable with the growth speed of the type-B edge if the BEP of Se is further decreased. Then the grown InSe domains come to have both type-A and type-B edges, and

becomes hexagonal.

If the flux intensity of Se is further decreased, a crossover of the growth speed occurs between the type-A edge and the type-B edge. When the BEP of Se is extremely low, the incorporation rate of Se atoms comes to determine the growth speed of the InSe domain. In this case the growth of the type-A edge is slower than that of the type-B edge, which results in the growth of triangular InSe domains surrounded by the type-A edges.

3-2. The attribution of two different kinds of domain edges

From the discussion in *Sec. 3-1*, *disordered* and *straight* edges in grown InSe domains can be identified as ‘type-A’ or ‘type-B’. When the BEP of Se was low, triangular InSe domains surrounded only by the disordered edges were observed by STM. From the results discussed above, these disordered edges are identified as the type-A edge. Contrary, the straight edges observed in the triangular InSe domain grown with a high Se BEP can be identified as the type-B edge.

3-3. Detailed structures of two different types of domain edges

As shown in STM images, the surface of the InSe domain is rather rough near the ‘type-A’ disordered edge, while it is very smooth near the ‘type-B’ straight edge. On every InSe domain, however, the surface near the domain center is smooth, and an atomic lattice image can be observed with a small

number of defect. We think these differences in the surface structure come from different reaction kinetics of In and Se atoms. It is supposed that excess Se atoms rapidly re-evaporate from the surface while In atoms remain on the surface at the substrate temperature of 340 °C. When the Se/In BEP ratio is small, these excess In atoms are likely to form defective regions deficient in Se atoms especially at the type-A domain edge, because this edge reacts with Se atoms more slowly than the type-B edge. Then, InSe domains are surrounded by the disordered type-A edges. As the growth proceeds, however, these defective regions can continue reacting with incoming Se atoms, and become stoichiometric InSe. Stoichiometric InSe has an inactive surface which no more react with incoming atoms. As a result triangular InSe domains with disordered domain edges grow, and they have an inner smooth surface and surrounding defective stripes, as shown in Fig. 3(a).

When the Se/In ratio is large enough, almost all In atoms react with Se atoms, and form stoichiometric InSe at 340 °C. In this case, however, excess Se atoms re-evaporate and do not remain on the substrate so that a defective structure lacking In atoms never grows. Then the triangular InSe domain has a smooth surface and type-B straight edges as shown in Fig. 3(c).

3-4. Determination of the position of In atoms relative to the topmost Se lattice

As shown in Fig. 1, the topmost Se layer of InSe has a six-fold lattice, and there are two possible positions where In atoms can be situated, ‘*b*-site’ or ‘*c*-site’

(Fig. 6(a)), if Se atoms possess *A*-sites. STM observes almost only the electronic structure of topmost Se atoms so that it is difficult to determine which site is occupied by In atoms in a given InSe island. The atomic-scale STM image of the InSe surface (Fig. 4) shows a close-packed hexagonal lattice which corresponds to the lattice of topmost Se atoms, but no systematic difference was recognized between *b*-sites and *c*-sites. It becomes possible, however, to determine the position of In atoms by examining STM images of the domain edge structure as discussed in the former sections. Now we can explicitly determine the type of the domain edge, type-A or type-B. If the type of domain edges is determined, the relative position of In atoms against Se atoms can be exclusively decided whether the *b*-site or the *c*-site. For example, if a triangular InSe domain which orients toward the upper direction has type-A disordered edges, then the stacking sequence of Se-In-In-Se atomic layers must be '*A-c-c-A*', as is shown in Fig. 6(b). Contrary, as shown in Fig. 6(c), if the domain is surrounded by type-B straight edges the stacking is determined to be '*A-b-b-A*'.

4. Conclusions

We made STM observations of III-VI compound semiconductor InSe sub-monolayer films, which were grown on MoS₂ substrates with various Se/In flux intensity ratios. It is found that the Se/In ratio affects the shape of InSe

domains, and the presence of two types of InSe domain edges, the straight edge and the disordered edge, is elucidated. It is observed that the medium Se/In ratio gives hexagonal InSe domains surrounded by alternate disordered and straight edges. Low Se/In ratio results in the growth of triangular InSe domains surrounded by only disordered edges, while InSe domains grown with high Se/In ratio become triangular ones surrounded only by straight edges. The change in the domain structure with the Se/In flux ratio can be explained by considering the crystal structure of InSe and the reaction kinetics of incoming In and Se atoms at two types of domain edges.

This work is supported by a Grant-in-Aid for Scientific Research from Ministry of Education, Science, Sports and Culture of Japan.

References

- [1] Z. Zhang and M. G Lagally (Eds.), *Morphological Organization in Epitaxial Growth and Removal* (World Scientific Publishing, Singapore, 1998)
- [2] W. K. Liu and M. B. Santos (Eds.), *Thin Films: Heteroepitaxial Systems* (World Scientific Publishing, Singapore, 1999)
- [3] A. Gousskov, J. Camassel and L. Gousskov, *Prog. Crystal Growth and Charact.* 5 (1982) 323.
- [4] J. A. Wilson and A. D. Yoffe, *Adv. Phys.* 18 (1969) 193.
- [5] A. Koma, K. Sunouchi and T. Miyajima, *J. Vac. Sci. Technol.* B3 (1985) 724.
- [6] K. Ueno, K. Saiki, T. Shimada and A. Koma, *J. Vac. Sci. Technol.* A8 (1990) 68.
- [7] A. Koma, *Thin Solid Films* 216 (1992) 72.
- [8] D. Fargues, L. B. Otsmane, M. Eddrief, C. Sébenne and M. Balkanski, *Appl. Surf. Sci.* 65/66 (1993) 661.
- [9] F. S. Ohuchi, T. Shimada, B. A. Parkinson, K. Ueno and A. Koma, *J. Cryst. Growth* 111 (1991) 1033.
- [10] R. Schlaf, D. Louder, O. Lang, C. Pettenkofer, W. Jaegermann, K. W. Nebesny, P. A. Lee, B. A. Parkinson and N. R. Armstrong, *J. Vac. Sci. Technol.* A13, (1995) 1761.
- [11] K. Ueno, K. Sasaki, N. Takeda, K. Saiki and A. Koma, *Appl. Phys. Lett.* 70 (1997) 1104.
- [12] K. Ueno, N. Takeda, K. Sasaki, and A. Koma, *Appl. Surf. Sci.* 113/114 (1997) 38.
- [13] J. Y. Emery, L. B. Otsmane, C. Hirlimann and A. Chevy, *J. Appl. Phys.* 71

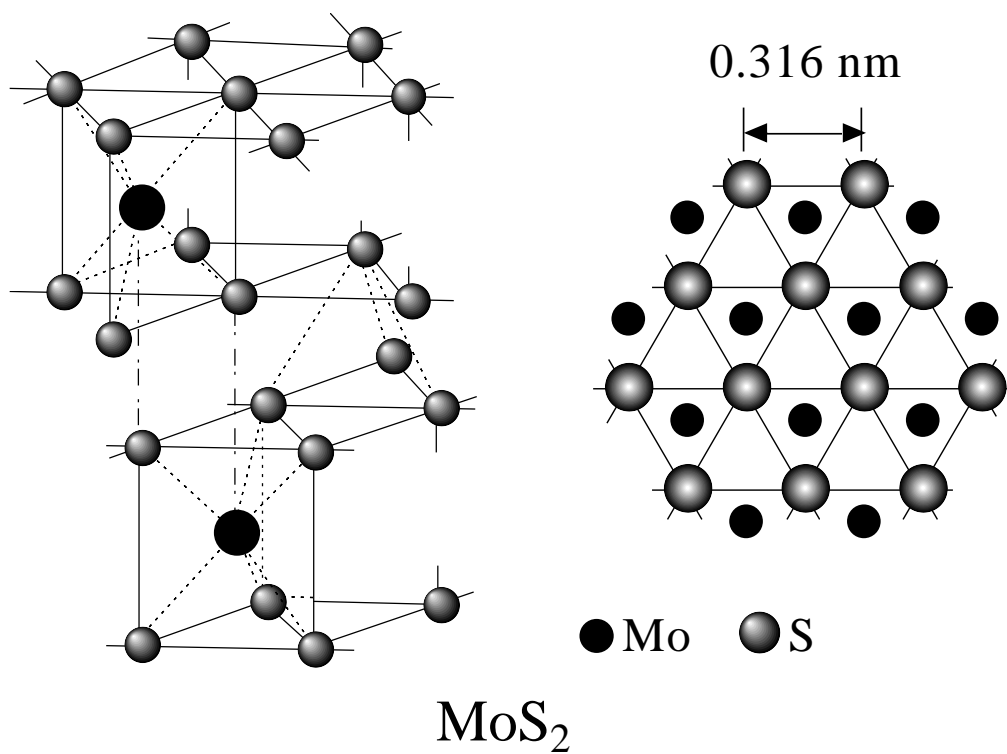
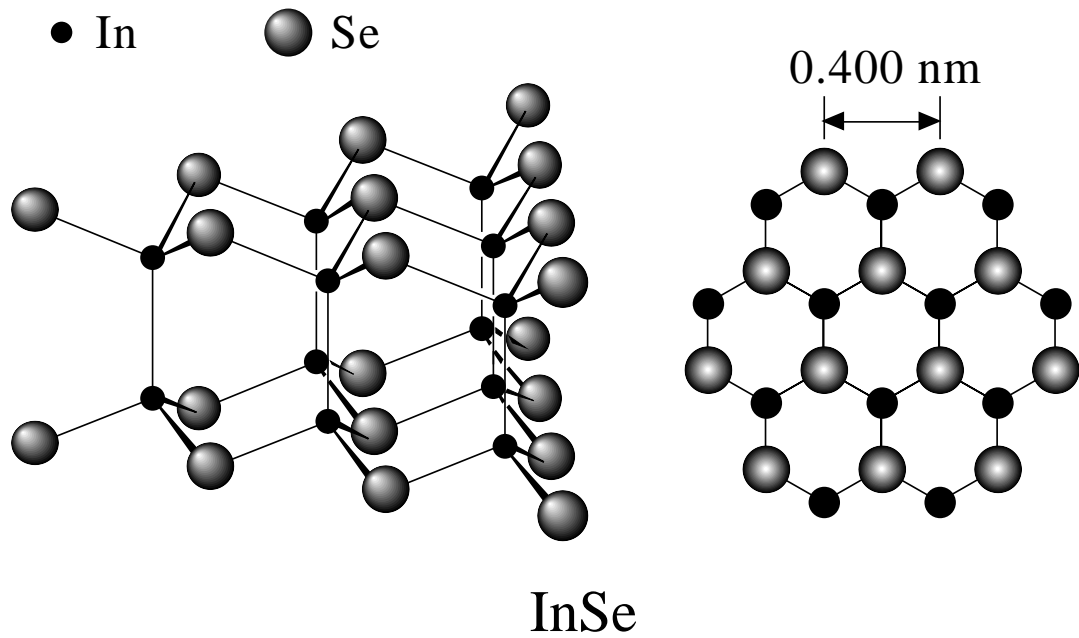
(1992) 3256.

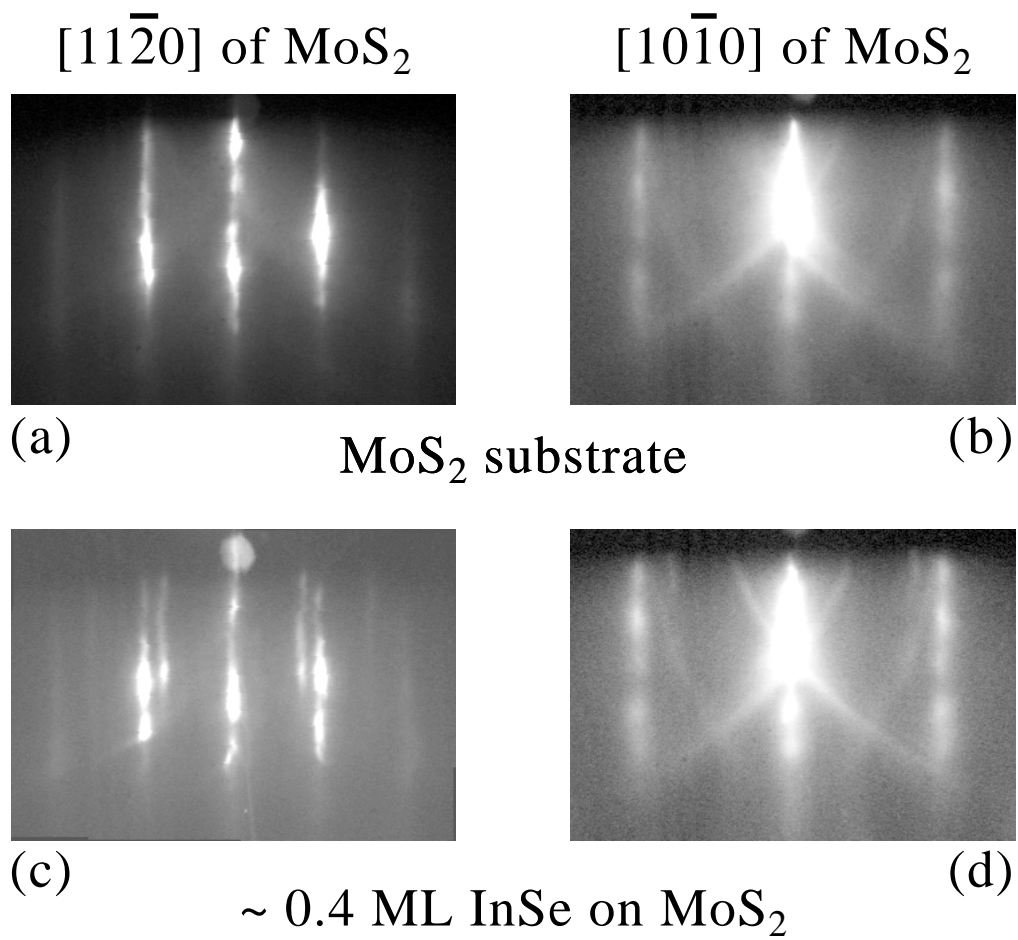
- [14] O. Lang, A. Klein, R. Schlaf, C. Pettenkofer, T. Löher, W. Jaegermann and A. Chevy, *J. Cryst. Growth* 146 (1995) 439.
- [15] K. Ueno, K. Sasaki, T. Nakahara and A. Koma, *Appl. Surf. Sci.* 130-132 (1998) 670.
- [16] K. Ueno, K. Sasaki, K. Saiki and A. Koma, *Jpn. J. Appl. Phys.* 38 (1999) 511.
- [17] J. Ye, Y. Nakamura and O. Nittono, *Philos. Mag.* A73 (1996) 169.

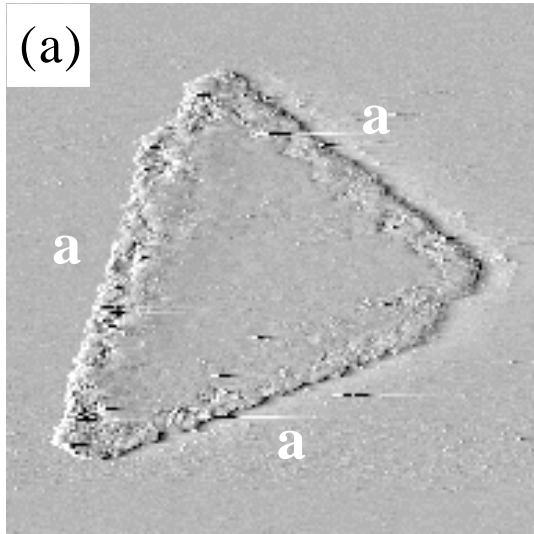
Figure captions

- Fig. 1 Perspective and top views of InSe (a) and MoS₂ (b).
- Fig. 2 RHEED patterns of a MoS₂ substrate (a, b) and an InSe film with ~ 0.2 ML coverage on the MoS₂ substrate (c, d). The direction of incident electron beam was set to be parallel to the $[1\bar{1}\bar{2}0]$ azimuth (a, c) or $[\bar{1}0\bar{1}0]$ azimuth (b, d) of the MoS₂ substrate, respectively.
- Fig. 3 STM images of InSe domains grown with different Se/In BEP ratios. The BEP of In was set to 3×10^{-6} Pa, and BEP of Se was changed to be (a) 2.0×10^{-5} Pa, (b) 5.0×10^{-5} Pa and (c) 2.0×10^{-4} Pa. Disordered ‘type-A’ edges are labeled as ‘a’, and smooth ‘type-B’ edges are labeled ‘b’. The sample bias voltage and the tunnel current were set to 0.8 V and 80 pA, respectively. Due to the anisotropy of the piezoelectric tube, STM images are distorted so that the triangular InSe domain in (c), for example, is not equilateral.
- Fig. 4 An atomic lattice image on the surface of InSe film grown on the MoS₂ substrate. The sample bias voltage and the tunnel current were set to -0.8 V and 80 pA, respectively.
- Fig. 5 A schematic view of the crystal structure of a hexagonal InSe domain indicating two different adjacent edges. Along the ‘type-A’ edge the incorporation rate of Se atoms is slower than the ‘type-B’ edge.
- Fig. 6 (a) Stacking positions of In and Se atoms in the hexagonal unit layer of InSe. When the topmost Se atoms occupy the ‘A’ positions, In atoms can be exclusively situated on ‘b’ or ‘c’ positions. (b), (c) Possible two stacking types in the upper-oriented triangular InSe domain. If the triangular InSe domain is surrounded by type-A edges, it should have the

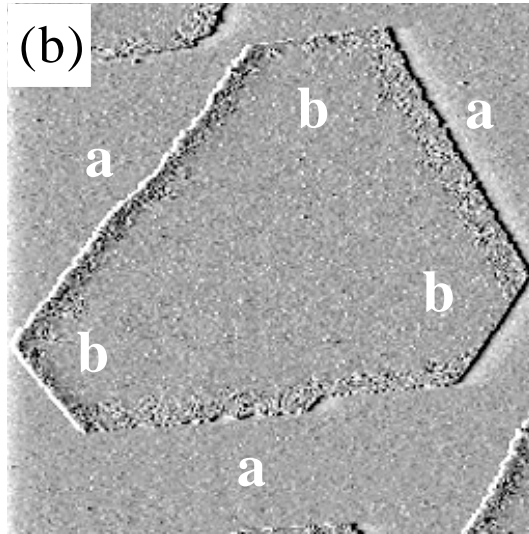
'*A-c-c-A*' stacking. If surrounded by 'type-B' edges, the '*A-b-b-A*' stacking is adequate.



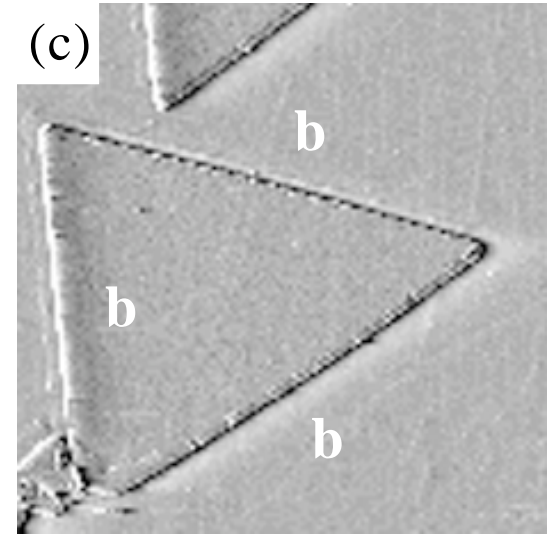




Se/In = 6.7
 $1000 \times 1000 \text{ nm}^2$



Se/In = 17
 $890 \times 890 \text{ nm}^2$



Se/In = 67
 $110 \times 110 \text{ nm}^2$

